Analytical Calculation of the Scattering Function for Polymers of Arbitrary Flexibility Using the Dirac Propagator

A. L. Kholodenko

375 H. L. Hunter Laboratories, Clemson University, Clemson, South Carolina 29634-1905

Received February 15, 1993; Revised Manuscript Received May 4, 1993

ABSTRACT: Using an earlier discovered analogy between Dirac's fermions and semiflexible polymers (*Ann. Phys.* (*N.Y.*) **1990**, *202*, 186), the static scattering function is calculated analytically for polymer chains of arbitrary stiffness and length. The obtained results are in excellent agreement with the available Monte Carlo data for semiflexible chains. On the basis of this agreement, a new method of measuring the persistence lengths is proposed.

1. Introduction

Although the conformational properties of semiflexible polymers had been studied experimentally for quite some time,[1] there has been very little progress of our theoretical understanding of these properties until recently. In particular, using the Kratky–Porod (K–P) model of semiflexible chains, Koyama[2] was able to calculate the first three even moments of the end-to-end distribution function. Using this information he made an attempt to calculate the scattering function $S(\mathbf{k})$. His $S(\mathbf{k})$ is in disagreement, however, with the exactly known[3] rigid-rod limit for $S(\mathbf{k})$ for arbitrary $\mathbf{k}$'s and coincides with rigid-rod $S(\mathbf{k})$ only asymptotically for $\mathbf{k} \to \infty$. In ref 4, $S(\mathbf{k})$ was calculated for the infinitely long (!) K–P chain, while in ref 5 the combination of analytical and numerical methods was used to obtain the results for chains of arbitrary length and flexibility. Because no useful closed-form analytical expression was obtained for $S(\mathbf{k})$, Monte Carlo methods were subsequently used to obtain $S(\mathbf{k})$ for chains of arbitrary flexibility (including the excluded-volume interactions in some cases). An up-to-date summary of the existing analytical and numerical results on $S(\mathbf{k})$ is given in ref 6. The failure of existing analytical approaches to calculate $S(\mathbf{k})$ in closed form is due to the difficulties of analytical calculations based on the K–P wormlike chain model.

In a series of papers[7–12] a new approach to conformational statistics of semiflexible polymers was developed. Being guided by the considerations of complementarity and consistency, this new approach allows one to preserve the results and methods traditionally used for the description of fully flexible polymers[13] and to extend them in a fully controllable way to chains of arbitrary flexibility. It is important to mention that this new method is not restricted to the single-chain properties. For example, in ref 8 Flory's[14] and Onsager's[15] results for solutions of semiflexible/ridid-rod polymers were reproduced and methods of obtaining systematic corrections to the above mean-field results were briefly discussed.

At the very foundation of our approach lies the observation made by Polyakov (e.g., see ref 16, p 225): "The geometrical properties of fermionic path are very different from bosonic one. In particular, while in the bosonic case we have a Brownian path with its size R and length L connected by the diffision law $R^2 \sim L$, in the Fermi case things are different, namely, $R^2 \sim L^2$."

Because fully flexible polymers are described by Brownian (bosonic) random walks at scales beyond the Kuhn's length[13] l (see below), then, upon rigidification, their description in terms of random walks becomes more and more fermionic in the sense given above. In refs 7 and 10, a precise mathematical description of the above bose–fermi transmutation is provided. It is based on the use of the Euclidean version of the Dirac propagator (instead of the Klein–Gordon propagator effectively used in fully flexible chain calculations[13]). In ref 12, $S(\mathbf{k})$ was calculated with the help of the Dirac propagator for chains of arbitrary length N and stiffness a (e.g., see eq 3.14 of ref 12). Subsequent analysis revealed (see also the text below) that eq 3.14 is acutally valid only in some limiting cases, e.g., for flexible chains ($a \ll N$) and for *all* chains for small $\mathbf{k}$'s. In this paper calculation of $S(\mathbf{k})$ for chains of arbitrary stiffness and for all k is presented.

2. Notations and Background

To introduce notations, consider the Fourier transformed end-to-end distance distribution function, $G(\mathbf{k},N)$. For the one-dimensional case ($d = 1$), it is given by:

$$G(\mathbf{k},N) = \int \mathrm{d}R\, e^{i\mathbf{k}\cdot R} G(R,N) \qquad (1)$$

With the help of eq 1, the moments are calculated, as usual, as

$$\langle \mathbf{R}^n \rangle = (-i)^n \left(\frac{\partial}{\partial \mathbf{k}}\right)^n G(\mathbf{k},N)\big|_{\mathbf{k}=0} \qquad (2)$$

For Gaussian chains in d-dimensions we have $G(\mathbf{k},N) \equiv G_0(\mathbf{k},N) = \exp(-\mathbf{k}^2 lN/2d)$, with $l = 2a$. The above identification $l = 2a$ follows from the K–P description of polymer chains and is valid, strictly speaking, only in the limit of small a's as discussed in detail in ref 12.

Using eq 2, we obtain, for example, $\langle \mathbf{R}^2 \rangle = Nl$. The scattering function $S(\mathbf{k})$ is obtained as[3,13]

$$S_0(\mathbf{k}) = \frac{1}{N^2}\int_0^N \mathrm{d}\tau \int_0^N \mathrm{d}\tau'\, G_0(\mathbf{k},|\tau-\tau'|) = \frac{2}{x^2}(x - 1 + e^{-x}) \qquad (3)$$

where $x = (\mathbf{k}^2/2d)Nl$.

Let us now examine the case of semiflexible chains. By continuity and complementarity, we expect the first equality in eq 3 to remain the same, with G_0 being replaced by a *yet unknown* distribution function $\hat{G}_0(\mathbf{k},|\tau|)$. To obtain $\hat{G}_0(\mathbf{k},|\tau|)$, it is helpful to recall that the function $S(\mathbf{k})$ is also known exactly in the rigid-rod limit.[3] In particular, for $d = 1$ it is given by[13] $S^{rr}(\mathbf{k}) = (\sin y/y)^2$, where $y = \mathbf{k}N/2$. Using eq 3 in *this* limit, we are faced with the problem of how to find $\hat{G}_0(\mathbf{k},|\tau|)$ if $S^{rr}(\mathbf{k})$ is known. If we try $\hat{G}_0(\mathbf{k},\tau) = \cos(\mathbf{k}\tau)$, then using eq 3 (with obvious replacements), we arrive at $S^{rr}(\mathbf{k})$ as required.

0024-9297/93/2226-4179$04.00/0

In refs 7 and 8 it was shown that for $d = 1$ the proper form for $\hat{G}_0(\mathbf{k},\tau)$ is

$$\hat{G}_0(\mathbf{k},\tau) = 2\cosh(mE\tau) + (2/E)\sinh(mE\tau) \quad (4)$$

It was explicitly demonstrated in refs 10 and 12 that $\hat{G}_0(\mathbf{k},\tau)$ *is* the Dirac propagator for a fictitious particle with mass $m \propto a^{-1}$ and $E^2 = 1 - \mathbf{k}^2/2m^2$. For $m \to 0$ (i.e., in the rigid-rod limit) and upon rescaling, $\tau \to 2^{1/2}\tau$ (e.g., see ref 9 for details), we obtain $\hat{G}_0(\mathbf{k},\tau) = 2\cos(\mathbf{k}\tau)$. The factor of 2 can be eliminated by introducing the normalized propagator $\hat{G}_n(\mathbf{k}\tau) = \hat{G}_0(\mathbf{k},\tau)/\hat{G}_0(0,\tau)$. Hence, *at least for $d = 1$*, the Dirac propagator, given by eq 4, reproduces known results for $S(\mathbf{k})$ in both the rigid-rod ($m \to 0$) and random-coil ($m \to \infty$) limits and *for chains of arbitrary stiffness* $S(\mathbf{k})$ is given in analytical form by eq 3.14 of ref 12. In order to extend the above result to the practically interesting 3D case, it is sufficient to perform an angular averaging of the above 1D result as explained in ref 17 (e.g., see sections 7.32 and 7.34). Indeed, in the case of rigid rods, if we replace y by $y\cos\Theta$ in $S^{rr}(\mathbf{k})$ given above, then, according to ref 17, we obtain

$$S(\mathbf{k}) = \langle S^{rr}(\mathbf{k})\rangle = \frac{1}{2}\int_{-1}^{1}\mathrm{d}(\cos\Theta)\left[\frac{\sin(y\cos\Theta)}{y\cos\Theta}\right]^2 = \frac{1}{y}\int_0^{2y}\frac{\sin x}{x}\,\mathrm{d}x - \left(\frac{\sin y}{y}\right)^2 \quad (5)$$

which is the well-known result[3] for the scattering function $S(\mathbf{k})$ for rigid rods in three dimensions. For completeness, it is instructive to demonstrate how the second line of eq 5 can be obtained form the first line. Begin with the observation that

$$2\frac{\sin(y\cos\Theta)}{y\cos\Theta} = \int_{-1}^{1}\mathrm{d}x\,\mathrm{e}^{ixy\cos\Theta} = \int_{-1}^{1}\mathrm{d}x\,\mathrm{e}^{-ixy\cos\Theta} \quad (6)$$

Using eq 6 we can rewrite the first line of eq 5 in the form

$$S(\mathbf{k}) = \frac{1}{2}\int_{-1}^{1}\mathrm{d}t\,\frac{1}{2}\int_{-1}^{1}\mathrm{d}x\,\frac{1}{2}\int_{-1}^{1}\mathrm{d}z\,\mathrm{e}^{-ity(x-z)} = \int_0^2\mathrm{d}x\int_0^2\mathrm{d}z\,\frac{\sin y(x-z)}{y(x-z)} = \frac{2}{N^2}\int_0^N\mathrm{d}x\,(N-x)\frac{\sin \mathbf{k}x}{\mathbf{k}x} \quad (7)$$

The last result coincides with that given by Yamakawa[3] for rods, as required, and leads directly[3] to the second line of eq 5. This result may be generalized for chains of arbitrary stiffness with the help of eq 3.14 of ref 12 and the angular averaging procedure just described. There is, however, an alternative way to arrive at the correct 3D result which is going to be demonstrated below.

3. Scattering Function from the Dirac Propagator

Begin with the observation that for rigid rods in 3D the angular averaged distribution function is known exactly[3] and is given by $\hat{G}(\mathbf{k},\tau) = (\sin \mathbf{k}\tau)/\mathbf{k}\tau$ (e.g., see eqs 3 and 7 above). When this result is substituted into eq 3 or eq 7, it produces the well-known $S(\mathbf{k})$ for rigid rods.[3] With the help of $\hat{G}(\mathbf{k},\tau)$ we can calculate the moments (e.g., $\langle\mathbf{R}^2\rangle$, etc.) by obvious generalization of eq 2 to the 3D case. This produces $\langle\mathbf{R}^2\rangle = N^2$, $\langle\mathbf{R}^4\rangle = (3/5)N^4$, etc. This should be contrasted with the K–P limiting results:[3] $\langle\mathbf{R}^2\rangle = N^2$ and $\langle\mathbf{R}^4\rangle = N^4$. Incidentally, notice that if we would formally use $\hat{G}_0(\mathbf{k},\tau) = \cos(\mathbf{k}\tau)$ in eq 2, then we would obtain $\langle\mathbf{R}^{2n}\rangle = N^{2n}$ for *all n*. In the opposite limit of random coils the situation is not better. Indeed, the K–P model produces $\langle\mathbf{R}^2\rangle = Nl$, $l = 2a$, and $\langle\mathbf{R}^4\rangle = (5/3)(Nl)^2$. The last result is in disagreement with that which could be obtained if we would use $G_0(\mathbf{k},N)$ in eq 2 (obviously generalized to the 3D case): for $\langle\mathbf{R}^4\rangle$ we would obtain $(Nl)^2$.

To obtain results which are in agreement with that which are exactly known for both limits, consider the Euclidean version of the 4D Dirac propagator[18] given by

$$G_{\mathrm{E}}(\mathbf{k},m) = \frac{-i}{\not{k} + m} = i\frac{\not{k} - m}{-\mathrm{k}^2 + m^2} \quad (8)$$

where, as usual, $\not{k} = \gamma^\mu \mathrm{k}_\mu$, with γ^μ being the usual Dirac matrices (Euclidean version) so that $\{\gamma^\mu,\gamma^\nu\} = -2\delta^{\mu\nu}$. Now let $m \to im$, then we obtain (by taking the trace)

$$\mathrm{tr}\,G_{\mathrm{E}} = \frac{m}{\mathbf{k}^2 + s^2 - m^2} \quad (9)$$

where s is the Laplace variable conjugate to "time", i.e., to the polymer's length. The inverse Laplace transform of tr G_{E} is given by

$$L^{-1}[\mathrm{tr}\,G_{\mathrm{E}}] = \frac{m}{(\mathbf{k}^2 - m^2)^{1/2}}\sin((\mathbf{k}^2 - m^2)^{1/2}N) \quad (10)$$

to be compared with eq 4. Let us normalize this expression to obtain

$$\hat{G}(\mathbf{k},N) = \frac{\dfrac{m}{(\mathbf{k}^2 - m^2)^{1/2}}\sin[(\mathbf{k}^2 - m^2)^{1/2}N]}{\sinh mN} \quad (11)$$

In accordance with the results of refs 7–12, consider the rigid-rod limit ($m \to 0$) of the above propagator. A simple calculation produces the result[3] for rigid rods. Consider now the opposite limit: $m \to \infty$ (which corresponds to random Gaussian coils). In this limit we obtain

$$\hat{G}(\mathbf{k},N) \approx \frac{\mathrm{e}^{-(\mathbf{k}^2/2m)N} - \mathrm{e}^{-2mN}\mathrm{e}^{(\mathbf{k}^2/2m)N}}{1 - \mathrm{e}^{-2mN}}\left(1 + \frac{\mathbf{k}^2}{2m^2}\right) \simeq \exp\left(-\frac{\mathbf{k}^2}{2m}N\right) \quad (12)$$

It is convenient now to rescale $m \Rightarrow \mathrm{d}m$ and to write (*in this limit only*), for such rescaled m, as $m^{-1} = l$. Then, we obtain $G_0(\mathbf{k},N)$ (e.g., see eq 2) as required. With the above-defined $\hat{G}(\mathbf{k},N)$ we can calculate moments such as $\langle\mathbf{R}^2\rangle$ in the way described in refs 7–12. For example, for $\langle\mathbf{R}^2\rangle$ we obtain ($d = 3$)

$$\langle\mathbf{R}^2\rangle_{\mathrm{D}} = \frac{N}{m}\left(\coth 3mN - \frac{1}{3mN}\right) \equiv \frac{4a^2}{3}xL(x) \quad (13)$$

where $L(x)$ is Langevin's function and $x = 3N/2a$ (which amounts to having $m^{-1} = 2a$ as before). Equation 13 is written in a form which is especially useful for comparison with $\langle\mathbf{R}^2\rangle$ for the K–P chains which is known to be

$$\langle\mathbf{R}^2\rangle_{\mathrm{K-P}} = 2a^2(y - 1 + \exp(-y)) \quad (14)$$

where $y = N/a$. In Figure 1 plots of $\langle\mathbf{R}^2\rangle$ for K–P and Dirac chains are depicted for some representative values of N. The corresponding radii of gyration are obtained in the usual way[3] as

$$\langle\mathbf{R}_{\mathrm{G}}^2\rangle = \frac{1}{N^2}\int_0^N\mathrm{d}x\,(N - x)\langle\mathbf{R}_x^2\rangle$$

A simple calculation produces

$$\langle\mathbf{R}_{\mathrm{G}}^2\rangle_{\mathrm{D}} = \frac{4a^2}{3}\frac{1}{x}\left[I_1(x) - \frac{1}{x}I_2(x)\right]$$

where $I_n(x) = \int_0^x\mathrm{d}z\,z^n(\coth z - 1/z)$, $n = 1, 2$. This be compared with the K–P result: $\langle\mathbf{R}_{\mathrm{G}}^2\rangle_{\mathrm{K-P}} = (a^2/\ldots$ $- 3y^{-1} + 6y^{-2} - 6y^{-3}(1 - \exp(-y))]$. Straightfor

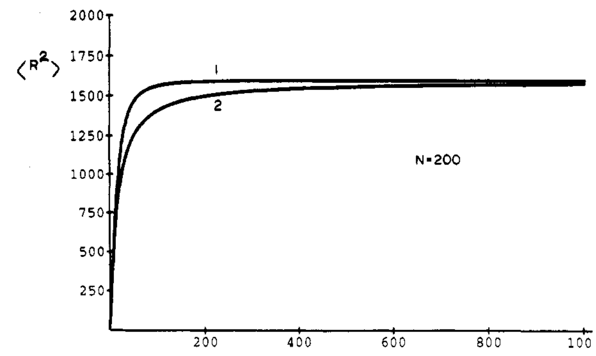

Figure 1. Mean-square end-to-end distance for Dirac (1) and K–P (2) chains as a function of persistence length a (for representative $N = 200$).

integration demonstrates that the corresponding radii of gyration behave practically the same as $\langle \mathbf{R}^2 \rangle$'s. Hence, for all practical purposes eqs 13 and 16 can be used *instead* of the corresponding K–P results. Moreover, in refs 7–12 it was demonstrated explicitly how K–P results for $\langle \mathbf{R}^2 \rangle$ and $\langle \mathbf{R}_G{}^2 \rangle$ can be obtained with the help of $\hat{G}_0(\mathbf{k},\tau)$ given by eq 4. Evidently, $\hat{G}_0$ given in eq 4 and $\hat{G}$ given in eq 11 are related to each other (see eq 19 and the following discussion). $\hat{G}$ provides, however, a *complete* description (for all $\mathbf{k}$'s, N's, and a's, see Figures 2–5) while $\hat{G}_0$ is only good for calculation of low moments of the distribution function, as was demonstrated in ref 12 where several observables (e.g., diffusion and viscosity coefficients) were calculated. Unlike the K–P case,[5] calculation of *all* moments is possible analytically now without any difficulties. Moreover, by combining eqs 3 and 11 the scattering function $S(\mathbf{k})$ is obtained which *by design* correctly reproduces the rigid-rod and random-coil limits and is given analytically by

$$S(\mathbf{k}) = \frac{2}{x}\left[I_{(1)}(x) - \frac{1}{x}I_{(2)}(x)\right] \tag{17}$$

where $I_{(n)} = \int_0^x dz\, z^{n-1} f(z)$, $n = 1, 2$; $x = 3N/2a$,

$$f(z) = \begin{cases} \dfrac{1}{E}\dfrac{\sinh(Ez)}{\sinh z} & (k \le 3/2\mathrm{a}) \\[2ex] \dfrac{1}{\hat{E}}\dfrac{\sin(\hat{E}z)}{\sinh z} & (k > 3/2\mathrm{a}) \end{cases}$$

and

$$E = \left[1 - \left(\frac{2}{3}a\mathbf{k}\right)^2\right]^{1/2} \quad \hat{E} = \left[\left(\frac{2}{3}a\mathbf{k}\right)^2 - 1\right]^{1/2}$$

The plots of $S(\mathbf{k})$ are presented in Figures 2 and 3. To better understand these plots, it is useful to recall that in the limit $k \to \infty$ $S(\mathbf{k})$ is expected to have the following asymptotic form:[4]

$$S(\mathbf{k}) \approx C_\infty(\mathbf{k}^2\langle \mathbf{R}_G{}^2\rangle)^{-1/2\nu} \tag{18}$$

In the case of rigid rods $C_\infty = \pi/12^{1/2}$, $\nu = 1$, and $\langle \mathbf{R}_G{}^2 \rangle = N^2/12$, while in case of random coils $C_\infty = 2$, $\nu = 1/2$, and $\langle \mathbf{R}_G{}^2 \rangle = 2aN/6$. In view of these results, it is useful to consider the combination $N\mathbf{k}^2S(\mathbf{k})$ as a function of $\mathbf{k}$. The results depicted in Figures 2 and 3 are useful to compare with the experimental plots of Krigbaum and Sasaki.[19] These authors have claimed that the use of small-angle X-ray scattering (instead of the usual light scattering) allows direct and quick measurement of the persistence length a. Being motivated by the asymptotic result (eq 18), they have observed a characteristic crossover from the random-coil (rc, horizontal line) to the rigid-rod (rr, positive slope line) behavior (e.g., see Figures 4 and 5 of

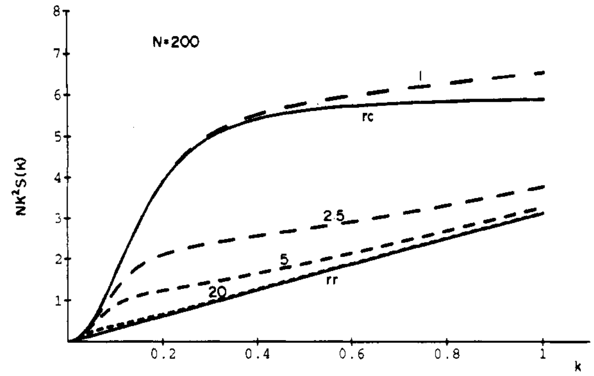

Figure 2. Plots of $N\mathbf{k}^2S(\mathbf{k})$ as function of $\mathbf{k}$ (for $N = 200$) for various values of persistence lengths a. $a = 1, 2.5, 5, 20, 50$, and 1000. The horizontal solid curve represents the random-coil (rc) asymptote for the Debye function while the solid positive slope curve corresponds to the rigid-rod (rr) asymptote. The curves for $a = 50$ and 1000 practically coincide with the rr asymptote.

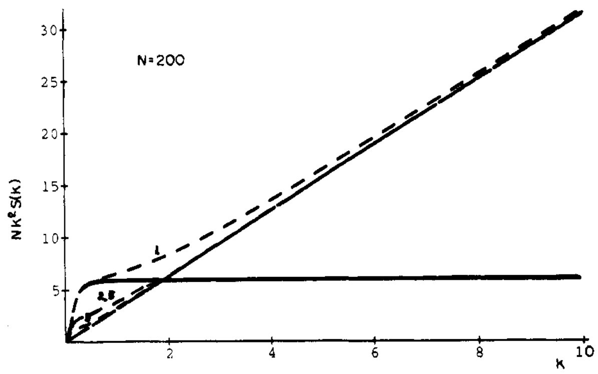

Figure 3. Same as Figure 2 but at a larger scale.

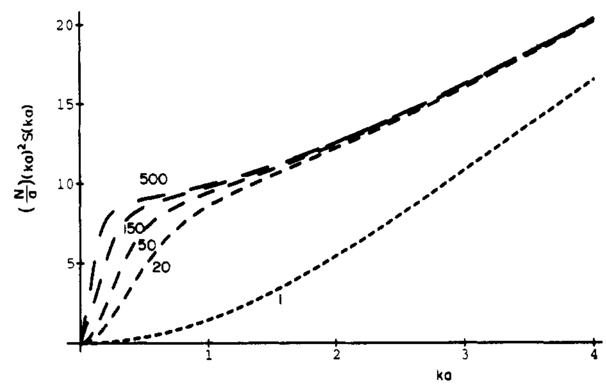

Figure 4. Normalized Kratky plot for the Dirac chain of various effective segment lengths N/a: rods $N/a \approx 1$ and coils $N/a > 50$.

ref 19). The results depicted in Figure 3 are in excellent agreement with that given in ref 11 for intermediate and large $\mathbf{k}$'s. However, unlike ref 19 (and ref 12) the results of Figure 3 do not indicate visible cusps at values of $\mathbf{k}$ determined from the equation $1 = (2/3)a\mathbf{k}^*$. The positions of cusps at $\mathbf{k}^*$'s were postulated to provide direct determination of the persistent length a. For small $\mathbf{k}$'s the amount of background noise is expected to be appreciable, as was acknowledged by the authors of ref 19, so that the measurement of $\mathbf{k}^*$ is rather unreliable. In view of that, Krigbaum and Brelsford[20] have alternatively suggested use of the normalized Kratky plot[21] (e.g., see Figure 8 of ref 20) to determine a. Based on eq 17, the Kratky plot for the Dirac chain is presented in Figure 4. The results are strikingly similar (if not identical!) to that obtained for a K–P chain (Figure 8 of ref 20) by Monte Carlo methods. It is equally striking to compare the results of our Figure 3 with Figure 7 of ref 22 and Figure 21 of ref 21. The above similarity of results is *the most vivid*

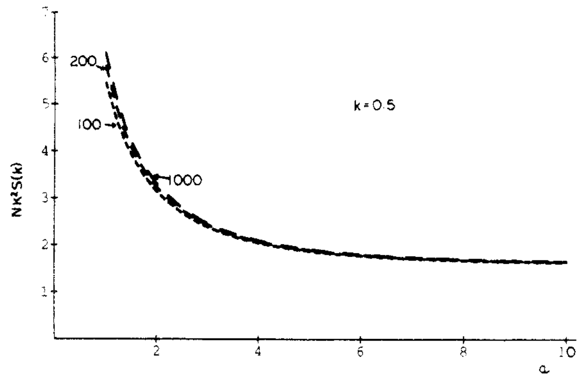

Figure 5. Plots of $Nk^2S(\mathbf{k})$ as a function of persistence length a for fixed value of $\mathbf{k}$ and various lengths N.

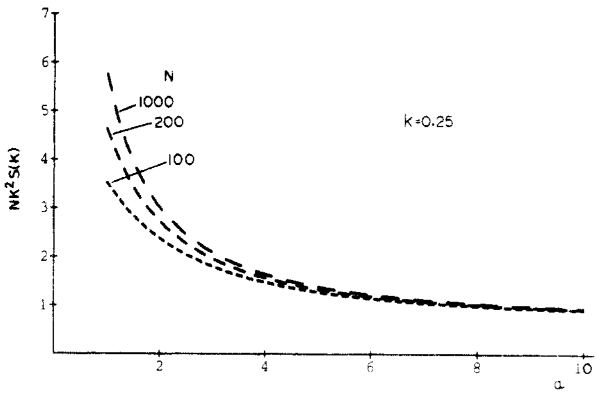

Figure 6. Same as in Figure 5 but for smaller $\mathbf{k}$'s.

manifestation of the bose–fermi transmutation discussed in the Introduction.

The Kratky plot (Figure 4) is not the most convenient way to determine a as was pointed out in ref 20. Figure 5 provides an alternative way of measuring a by plotting the experimentally measurable combination $N\mathbf{k}^2S(\mathbf{k})$ versus a for fixed wavelength $\mathbf{k}$. As Figure 5 indicates, this plot is rather insensitive to the chain length N and therefore is universal. The numerical analysis of eq 17 shows that this remains true for as long as $\mathbf{k}$ is not too small. Taking into account that the excluded-volume effects leave $S(\mathbf{k})$ practically unchanged (e.g., see Figures 2 and 4 of ref 23), the plot of Figure 5 can serve as a useful alternative to the Kratky plot which, in addition, does not suffer from the polydispersity effects.

The results of Figure 5 should be contrasted with that of Figure 6 which depicts the same plot but for smaller values of the wavevector $\mathbf{k}$. Obviously, making measurements at larger $\mathbf{k}$'s dramatically reduces the effects of both the polydispersity and the excluded volume on the accuracy of measurements of a.

4. Discussion

It is important now to understand better the interrelation between the propagators given by eqs 4 and 11. The Laplace transformed version of eq 4 is known[12] to be (upon obvious rescaling)

$$\frac{1}{2}\hat{G}_0(\mathbf{k},s) = \frac{s+m}{\mathbf{k}^2 + s^2 - m^2} \tag{19}$$

This is to be compared with eq 9. Equation 19 can be obtained with help of the Dirac propagator (eq 8). Indeed, as discussed in refs 8 and 9, the lattice version of the propagator $\hat{G}_0$ is obtained only if proper averaging over the initial states and summation over the final states of the lattice walk is done, as is also done in the case of the continuous limit for the Dirac particle.[24] In the continuous limit the polarization density matrix ρ is used (e.g., we can choose $\rho = (1/4)/(I + \gamma^{\mu}a_{\mu}))$ so that tr $\rho = 1$ and a_{μ} can be assigned to properly account for the orientation of the initial and final states. If we choose ρ in the form $\rho = (1/4)(I + i\gamma^4)$, then multiplying of both sides of eq 8 by ρ and taking the trace brings us back to eq 19 as required. It is important to notice that the above averaging of the initial and final states is also crucially required for the bosonic K–P propagator discussed in ref 8.

In conclusion, several comments can be made. First, the above results are also of interest in particle physics[25] where for quite some time attempts have been made to construct the path integrals for relativistic particles with spin by means of bosonic Lagrangian with higher derivatives. The models considered so far[26] contain the tachyons (i.e., particles with imaginary masses) which are apparently of no physical interest. However, eqs 8 and 9 indicate that in statistical mechanics of polymers the situation is just the opposite. Extension of the above one-dimensional models to two-dimensional models for the semiflexible surfaces[8] might require use of the tachyonic states as well. This could be understood by considering the conformational properties of the K–P–Dirac curve lying on the fluctuating semiflexible surface. These ideas are currently under development.[27] Second, in ref 8 it was indicated that the analogy between the K–P and Dirac path integral formulations of semiflexible chains is *not* one-to-one (e.g., see Figure 1) so that the moments of distribution functions are different in general. This difference is not significant, however, as the above-presented results demonstrate, but the consistency requirements discussed in this paper strongly favor the Dirac description (fermionic or bosonic(!)) versus the conventional K–P. Third, from the results on semiflexible polymers already obtained, it is possible to conclude that the effects of the excluded volume[11] on the conformational characteristics of polymer chains can be mimicked by the appropriate choice of the persistence length a. In the case of self-avoiding surfaces, the same idea has also been recently discussed in ref 28. There it was shown that the effects of surface self-intersections can be transformed into an extra rigidity term in the surface path integral, thus converting the integral for the flexible (bosonic) string into a Polyakov–Kleinert "smooth" string[16,29] path integral.

Acknowledgment. I thank Dan Bearden (Clemson), Jack Douglas (NIST), Vladimir Nesterenko (JINR, Dubna, Russia), Christopher Reed (Tulane), Hagen Kleinert (Berlin), and Thomas Vilgis (Mainz) for helpful communications.

Note Added in Proof: After this paper was accepted for publication, I was kindly informed by Dr. Vilgis that he had used earlier the relativistic Klein–Gordon propagator for description of conformational properties of polymer chains. In ref 30 he had obtained the first correction to G_0, eq 2, caused by the effects of rigidity.

References and Notes

(1) Tsvetkov, V. *Rigid Chain Polymers*; Plenum Press: New York, 1989.
(2) Koyama, R. *J. Phys. Soc. Jpn.* **1973**, *34*, 1029.
(3) Yamakawa, H. *Modern Theory of Polymer Solutions*; Harper and Row: New York, 1971.
(4) des Cloizeaux, J. *Macromolecules* **1973**, *6*, 403.
(5) Yamakawa, H.; Fujii, M. *Macromolecules* **1974**, *7*, 649.
(6) Reed, C.; Reed, W. *J. Chem. Phys.* **1992**, *97*, 7766.
(7) Kholodenko, A. *Phys. Lett. A* **1989**, *141*, 351.

(8) Kholodenko, A. *Ann. Phys. (N.Y.)* **1990**, *202*, 186.
(9) Kholodenko, A. *J. Stat. Phys.* **1991**, *65*, 291.
(10) Kholodenko, A. *Phys. Lett. A* **1991**, *159*, 437.
(11) Kholodenko, A. *J. Chem. Phys.* **1991**, *95*, 628.
(12) Kholodenko, A. *J. Chem. Phys.* **1992**, *96*, 700.
(13) des Cloizeaux, J.; Jannink, J. *Polymers in Solutions: Their Modelling and Structure*; Clarendon Press: Oxford, U.K., 1990.
(14) Flory, P. *Proc. Soc. London* **1956**, *234*, 60.
(15) Onsager, L. *Ann. N.Y. Acad. Sci.* **1949**, *51*, 627.
(16) Polyakov, A. *Gauge Fields and Stings*: Harwood Academic: New York, 1987.
(17) Van de Hulst, H. *Light Scattering by Small Particles*; John Wiley and Sons, Inc.: New York, 1957.
(18) Ramond, P. *Field Theory: A Modern Primer*, Addison-Wesley: New York, 1989.
(19) Krigbaum, W.; Sasaki, S. *J. Polym. Sci., Polym. Phys. Ed.* **1981**, *19*, 1339.
(20) Brelsford, G.; Krigbaum, W. In *Liquid Crystallinity in Polymers*; Ciferi, A., Ed.; VCH Publishers, Inc.: New York, 1991; Chapter 2.
(21) Glatter, O.; Kratky, O. *Small Angle X-Ray Scattering*; Academic Press: New York, 1982; Chapter 12.
(22) Kirste, R. In *Small Angle X-Ray Scattering*; Brumberger, H., Ed.; Gordon and Breach: New York, 1967; Chapter 3.
(23) Ohta, T.; Oono, Y.; Freed, K. *Phys. Rev.* **1982**, *A25*, 2801.
(24) Berestetskii, V.; Lifshiftz, E.; Pitaevskii, L. *Quantum Electrodynamics*; Pergamon: Oxford, U.K., 1982.
(25) Nesterenko, V. (JINR, Dubna, Russia) Private communication.
(26) Nesterenko, V. *Classical Quantum Gravity* **1992**, *9*, 1101.
(27) David, F. *Nucl. Phys.* **1992**, *B368*, 671.
(28) Karanikas, A.; Ktorides, C. *Phys. Lett.* **1990**, *B235*, 90.
(29) Polyakov, A. *Nucl. Phys.* **1986**, *B268*, 406. Kleinert, H. *Phys. Lett.* **1986**, *B174*, 335.
(30) Vilgis, Th.; Kilian, H. *Colloid Polym. Sci.* **1986**, *264*, 131.